

The 43rd RD50 Collaboration Workshop
30 November 2023

Investigation of low gain avalanche detectors exposed to proton fluences beyond $10^{15} n_{eq}/cm^2$

Josef Sorenson, Martin Hoeferkamp, Sally Seidel, Jiahe Si

University of New Mexico

Gregor Kramberger

Jozef Stefan Institute

arXiv:2311.02027 [physics.ins-det] (submitted to JINST)

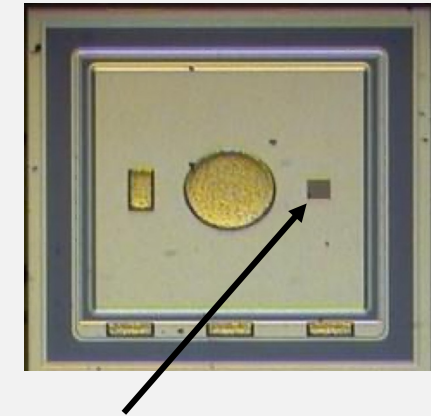
LGADs used in this study: HPK2

- Two sets of LGADs are used in this study: the second production by Hamamatsu Photonics K.K. (HPK2) and the fourth production by Fondazione Bruno Kessler (FBK4)
- Both sets include single LGAD sensors, LGAD sensors fabricated in 2x2 arrays (QUAD), and single sensors fabricated without a gain layer (PIN).

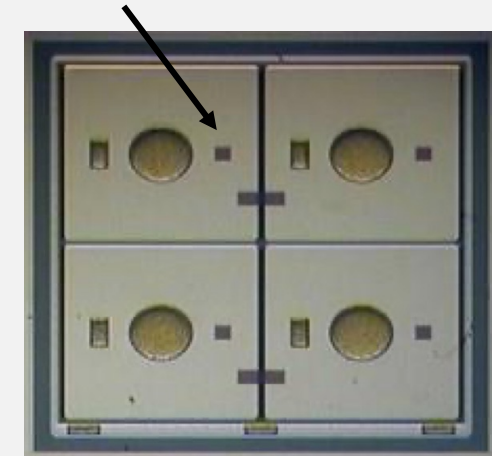
LGADs used in this study: HPK2

- n^{++} (electrode) – $1.3 \times 1.3 \text{ mm}^2$
- p^+ (gain layer) – $0.7 \text{ }\mu\text{m}$ thickness, $1.8 \text{ }\mu\text{m}$ depth
- $50 \text{ }\mu\text{m}$ thick active layer
- $200 \text{ }\mu\text{m}$ total thickness
- single guard ring
- epitaxial Si grown on Czochralski substrate
- Four different gain layer doping profiles. Profile 1 has the lowest concentration and Profile 4 has the highest.

HPK2 Wafer ID	Gain Layer Doping Profile	$V_{gl,0}$ [V]	$V_{fd,0}$ [V]
25	1	53.0	55.0
31	2	52.0	54.0
36, 37	3	49.5	52.0
42, 43	4	49.0	51.0

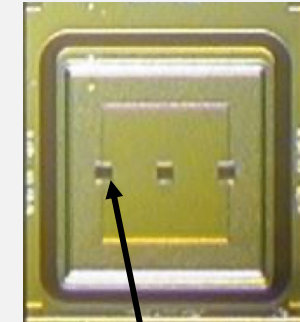


Optical windows for laser measurements

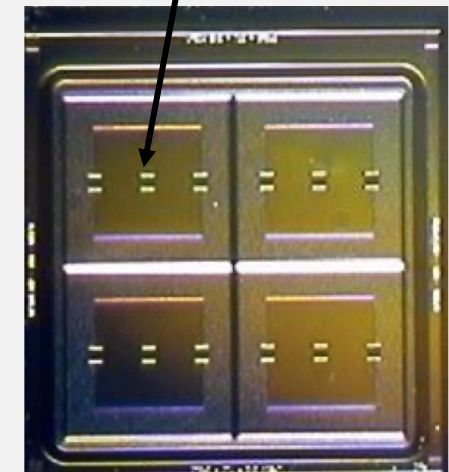


LGADs used in this study: FBK4

- n^{++} (electrode) – 1.3 x 1.3 mm²
- p^+ (gain layer) – 0.7-2 μm thick
- The depth of the gain implant varies in different samples (1-2 μm).
- 55 μm thick active layer
- Multiple guard rings
- Different gain layer dopant profiles and concentrations
- **Carbon co-implantation in the gain layer is used to improve radiation resistance. The carbon dose varies in different samples.**



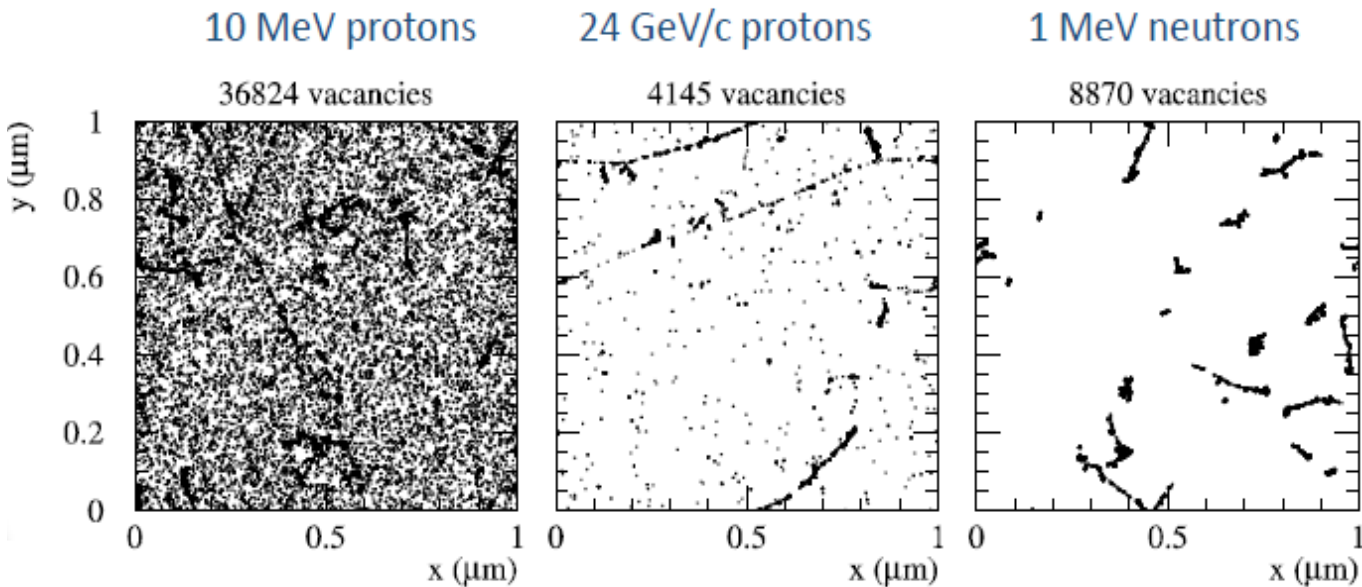
Optical windows for laser measurements



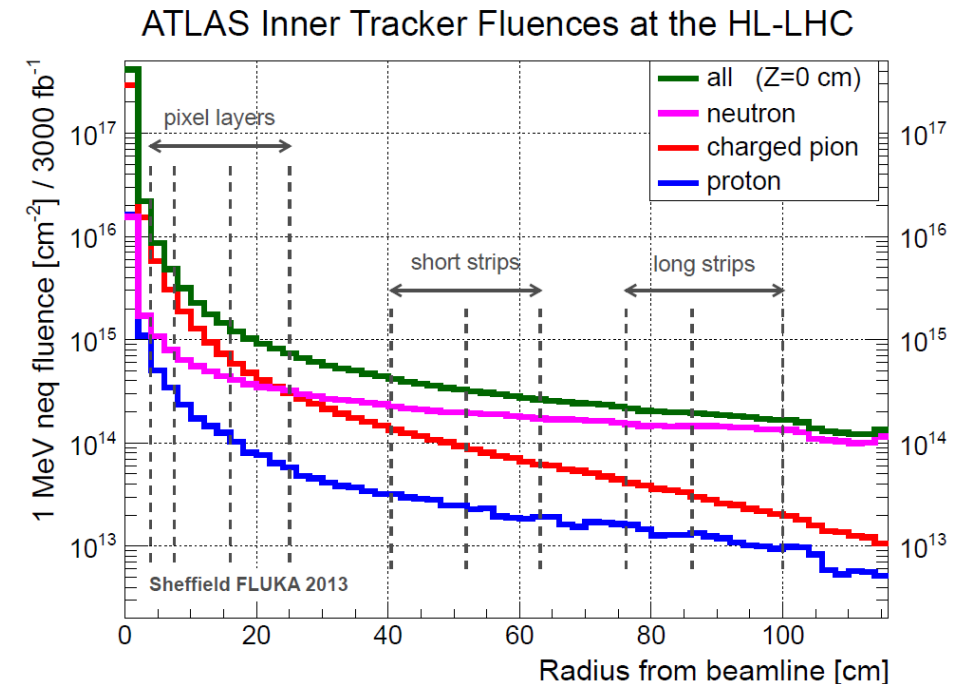
FBK4 Wafer ID	Gain Layer Depth	Relative Boron Concentration	Relative Carbon Concentration	Diffusion	$V_{gl,0}$ [V]	$V_{fd,0}$ [V]
1	Shallow	0.98	0.6	CH-BL	21.5	23.0
2	Shallow	1.02	1	CH-BL	22.0	23.5
5	Shallow	1.04	1	CH-BL	22.5	24.0
9	Shallow	1.06	1	CH-BL	22.5	24.5
12	Deep	0.77	0.6	CH-BH	50.5	51.5
16	Deep	0.81	0.6	CL-BL	48.0	49.0
18	Deep	0.93	0.6	CL-BL	48.5	49.5

Importance of proton irradiations

- A non-negligible fraction of the fluence in the HGTD and ETL will be from charged pions and protons. Proton irradiations are the subject of this study.
- The characteristics of radiation damage depend on both the particle type and energy, and are not fully accounted for in the NIEL scaling hypothesis.
- Every result presented in this talk is scaled using NIEL to the 1 MeV neutron equivalent damage (n_{eq}).

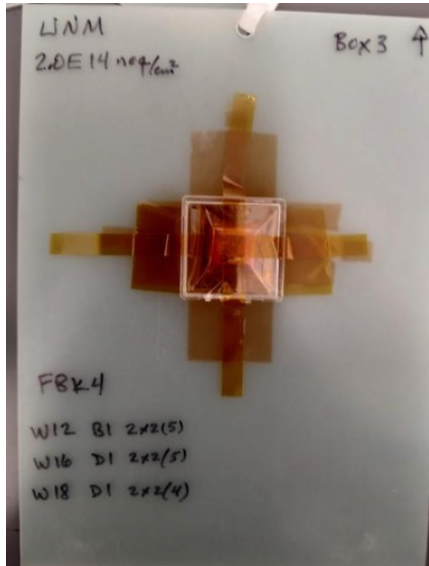


[Mika Huhtinen NIMA 491(2002) 194]

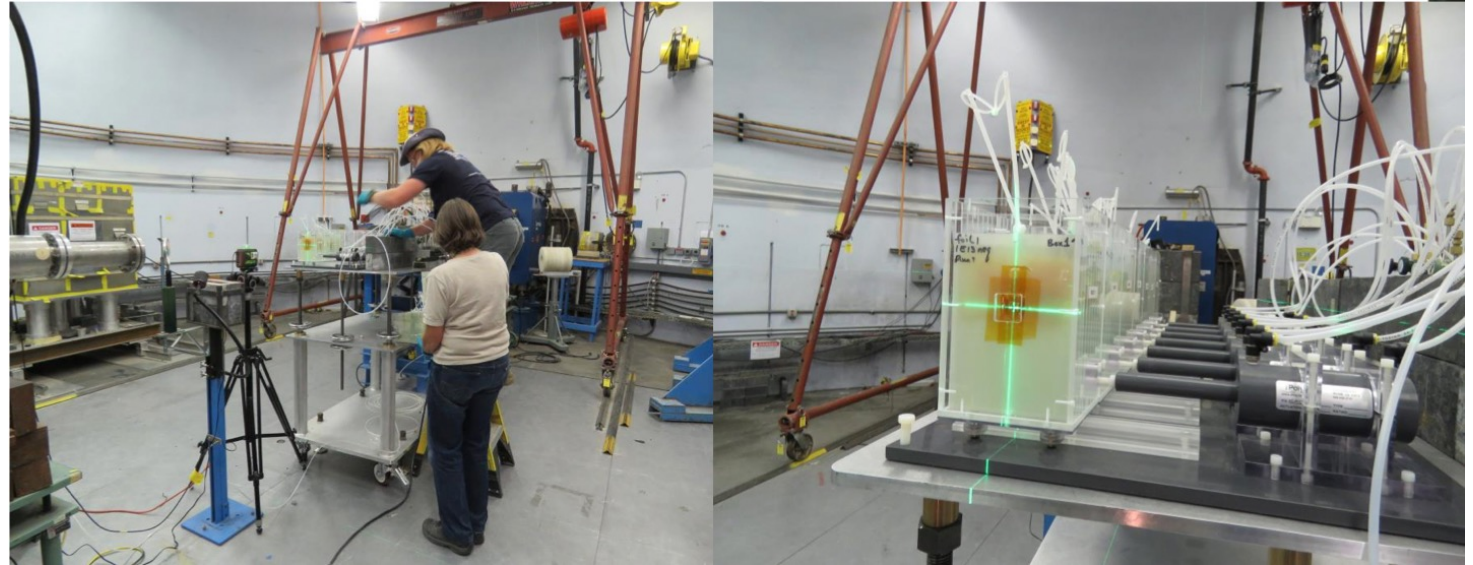


Irradiation Campaigns

- This study includes two different irradiation campaigns: (1) the FBK4 sensors were irradiated at the Fermilab Irradiation Test Area (FNAL-ITA) with 400 MeV protons and (2) the HPK2 sensors were irradiated at the Los Alamos Neutron Science Center (LANSCE) with 500 MeV protons.
- For 400 MeV and 500 MeV protons the hardness factors are 0.83 and 0.78 respectively.
- The irradiated samples are kept in a freezer at -25°C to prevent unintentional annealing. All the sensors are subjected to a standard annealing regimen of 60°C for 80 minutes.



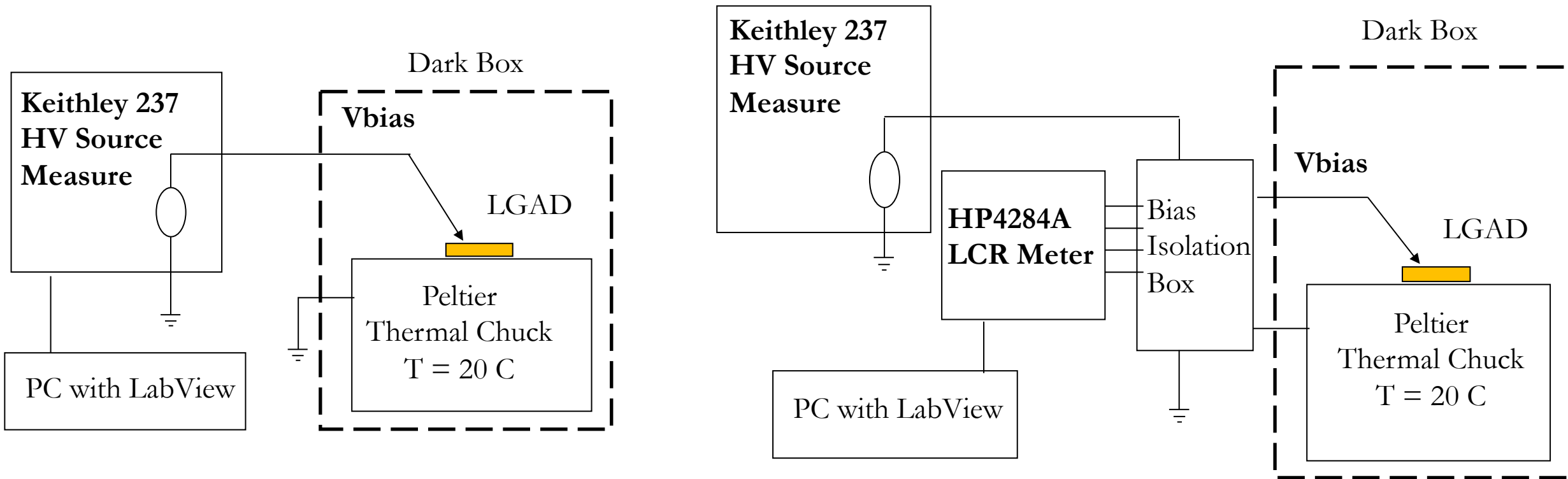
LGADs mounted on G10 Board



Irradiation hall at LANSCE

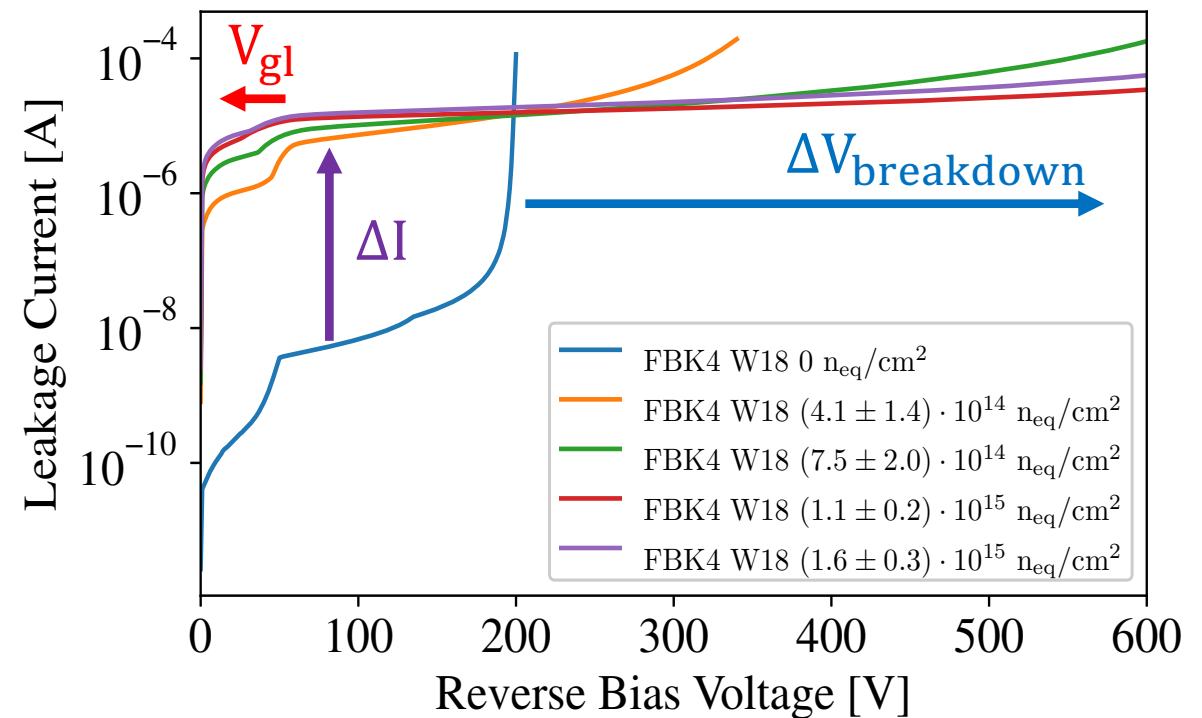
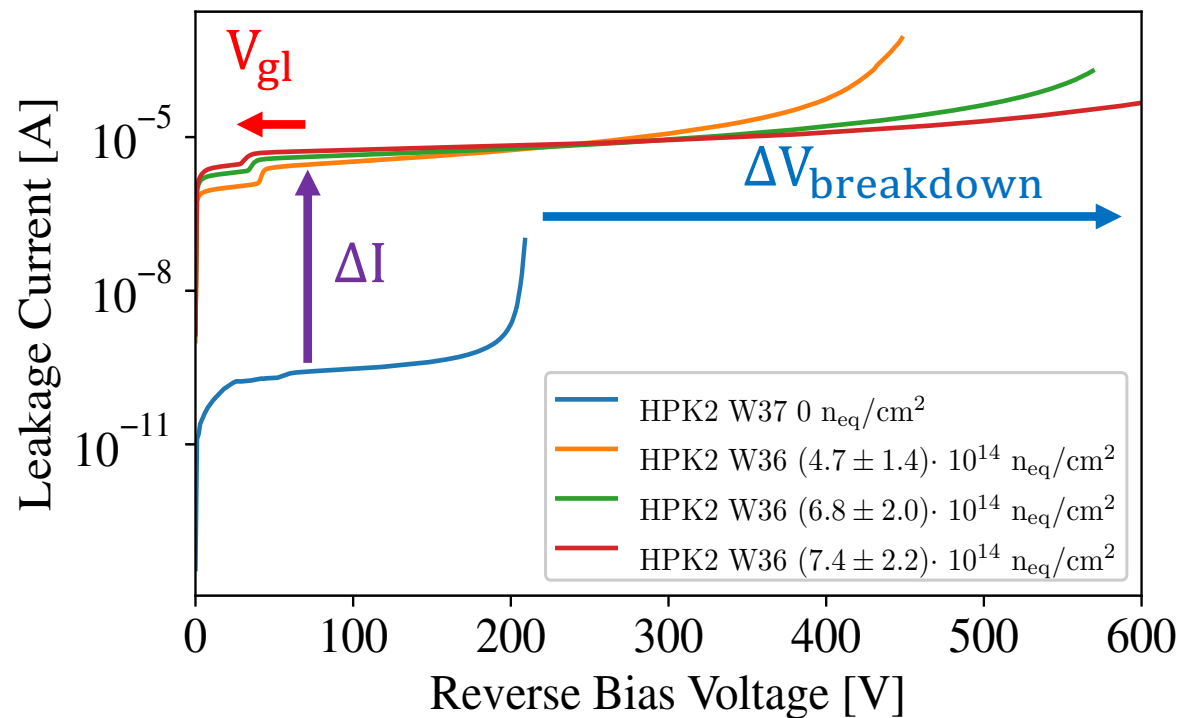
IV and CV measurements

- IV measurements are used to infer the leakage current and breakdown voltage of LGADs.
- CV measurements are used to infer the gain layer depletion voltage, V_{gl} , and the full depletion voltage, V_{fd} .



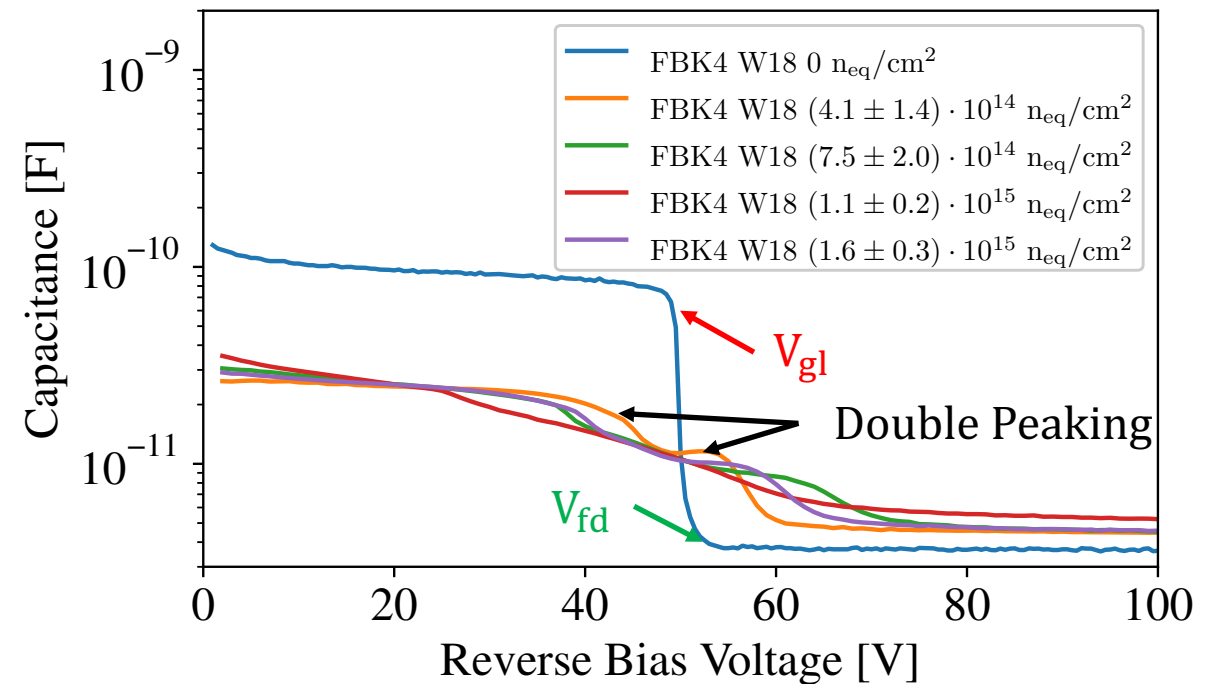
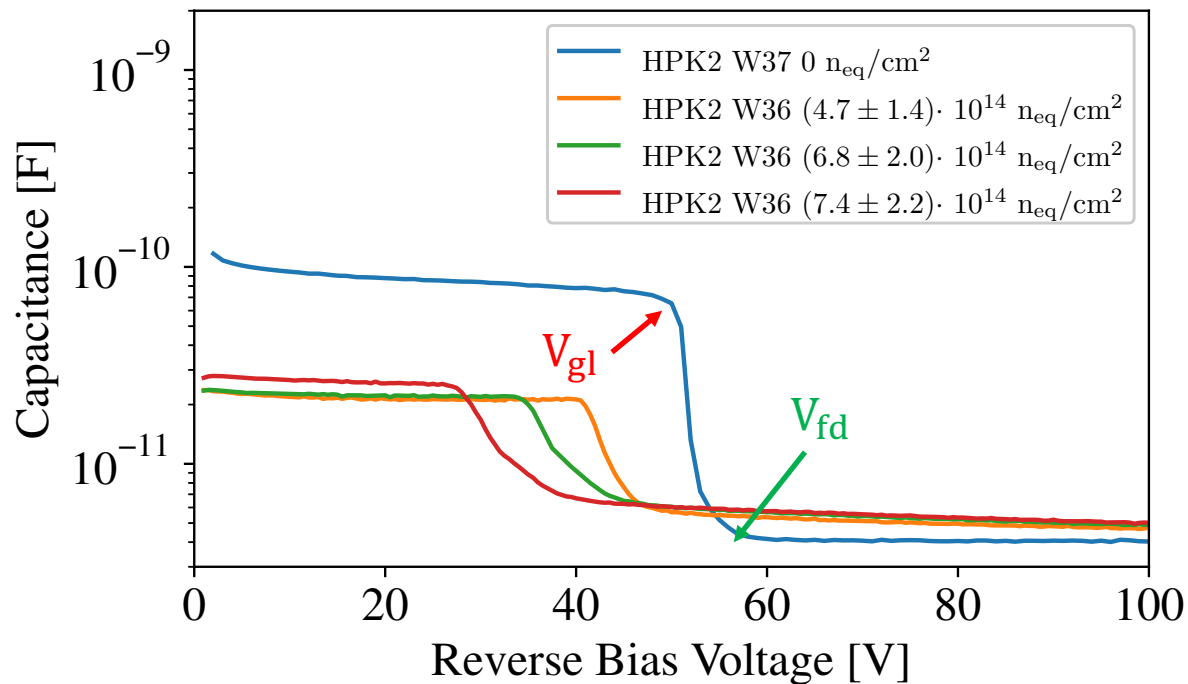
IV Measurement Results

- IV measurements were made for all wafers. Here are examples for the FBK4 and HPK2.
- The increase in leakage current, ΔI , and breakdown voltage, $\Delta V_{\text{breakdown}}$, increases with fluence for both sensors.
- At the gain layer depletion voltage, V_{gl} , there is a small jump in the leakage current.



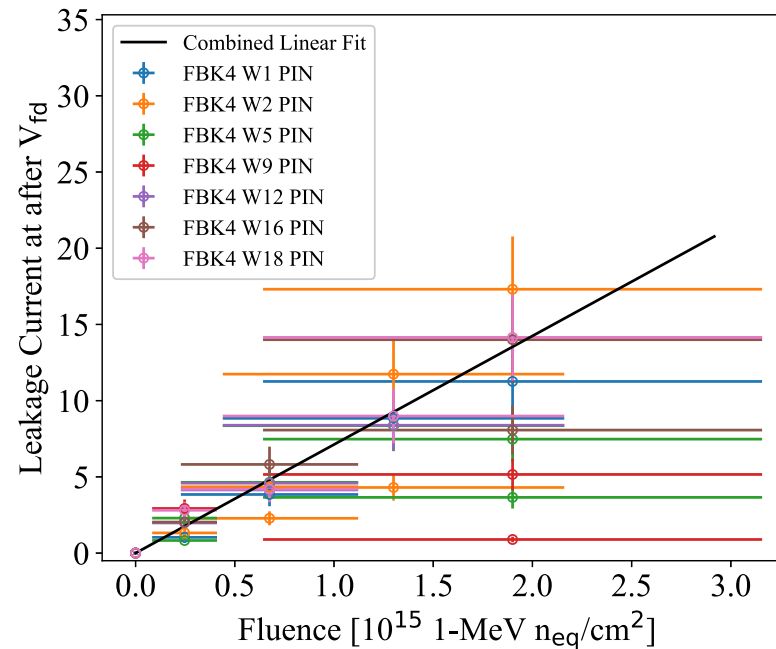
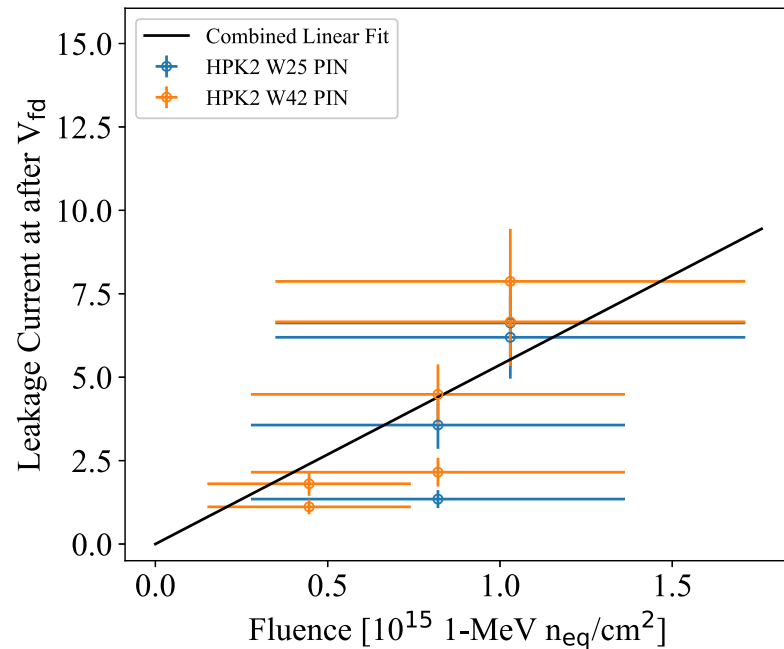
CV Measurement Results

- CV measurements were made for all wafers. Here are examples for the FBK4 and HPK2.
- The voltage where the gain layer is depleted, V_{gl} , is shown by the first drop in capacitance.
- The voltage where the full sensor is depleted, V_{fd} , is shown where the capacitance flattens after dropping.
- The FBK sensors show a double peaking behavior in their capacitance after the proton irradiations that we would like to understand better.



Damage Constant from PIN sensors and Fluence Scaling

- The leakage current increases linearly with fluence, according to $\Delta I = \alpha \cdot \phi \cdot Vol$ where α is the damage constant, ϕ is the fluence, and Vol is the volume of the sensor.
- PIN sensors are used to extract α because they do not have gain.
- The leakage current is extracted at 5 volts above the PIN sensor full depletion voltage.
- The errors in fluence and leakage current are considered in the fit and propagate into the error in α .



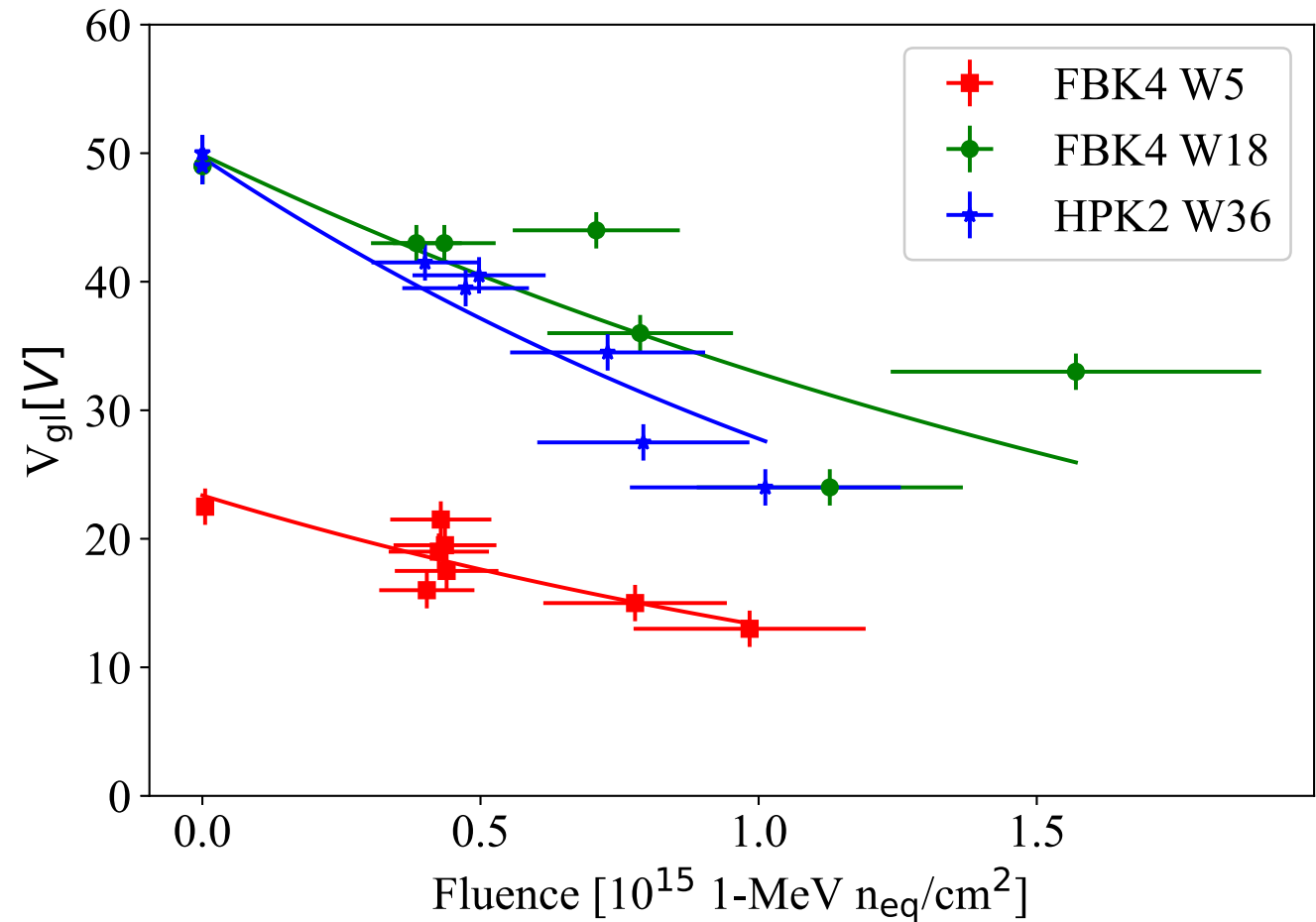
$$\alpha_{HPK2} = (5.3 \pm 0.7) \cdot 10^{-17} \text{ A/cm}$$

$$\alpha_{FBK4} = (6.9 \pm 0.4) \cdot 10^{-17} \text{ A/cm}$$

These α values are used to calculate the fluence received by the LGADs

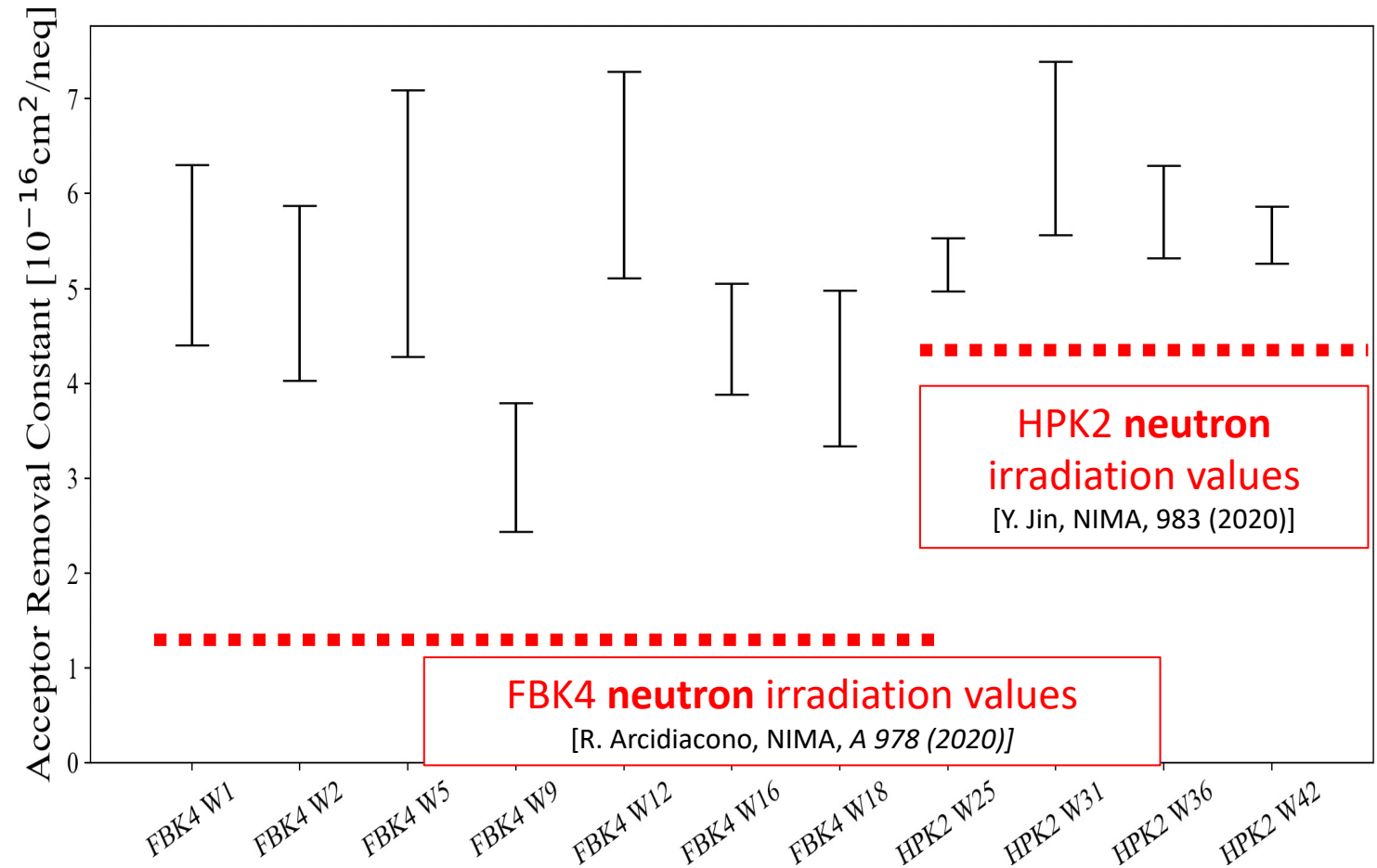
Application of IV and CV measurements to evaluate gain layer acceptor removal

- An algorithm for extracting the V_{gl} based on both the CV and IV measurements is used on each wafer.
- A decaying exponential, $V_{gl}(\phi) = V_{gl,0} \cdot e^{-c \cdot \phi}$, is fit to V_{gl} vs fluence data to extract the acceptor removal constant, c .
- An example of this fit for a few of the wafers is shown to the right.



Acceptor Removal Comparison

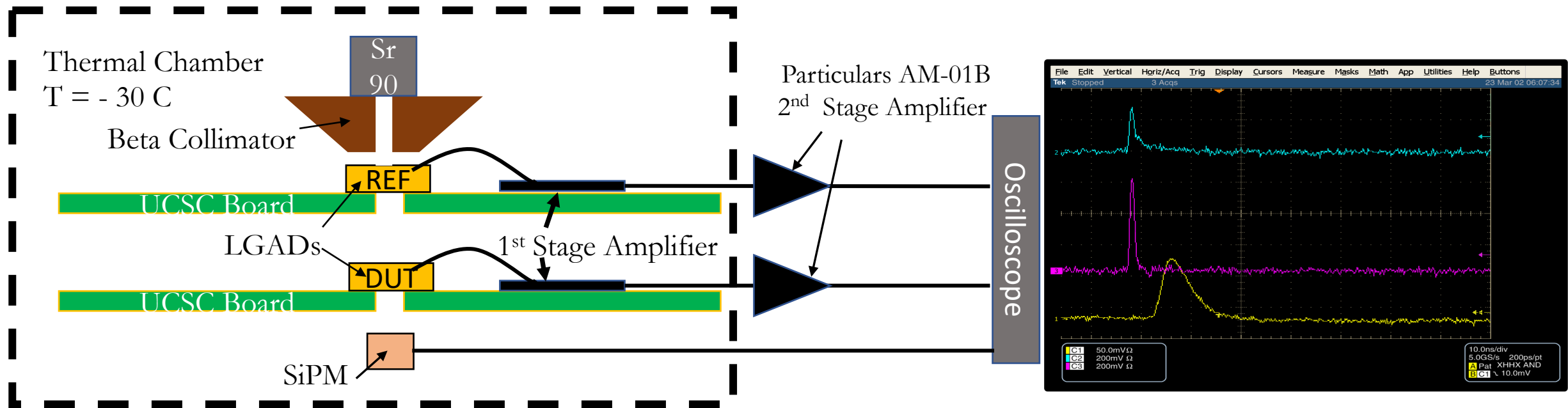
- The 400/500 MeV proton irradiated acceptor removal constant values are higher than for neutron irradiations on the same type of sensors.
- The acceptor removal constant for each wafer measured is shown in the chart on the right.
- The carbon co-implanted FBK4 W9 prototype has the lowest value.



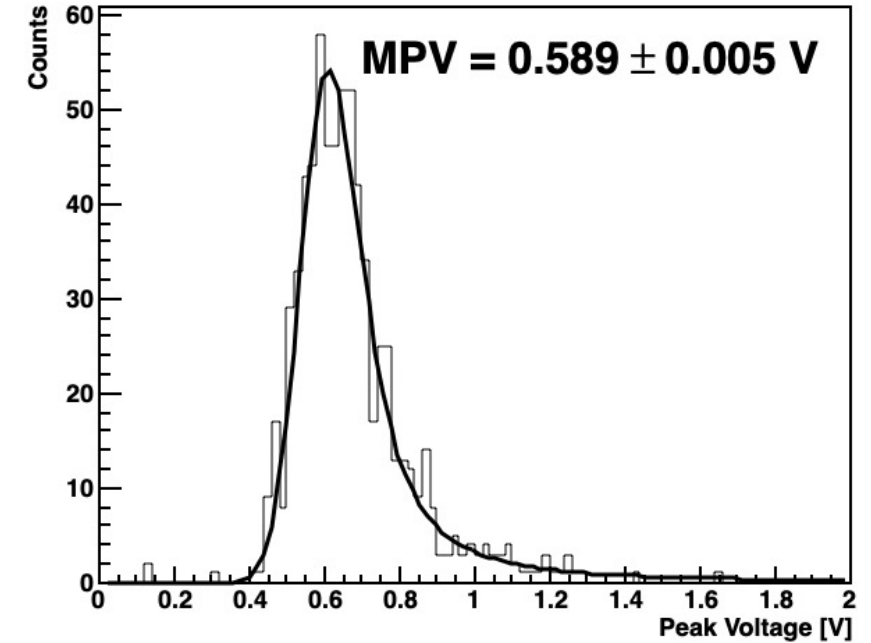
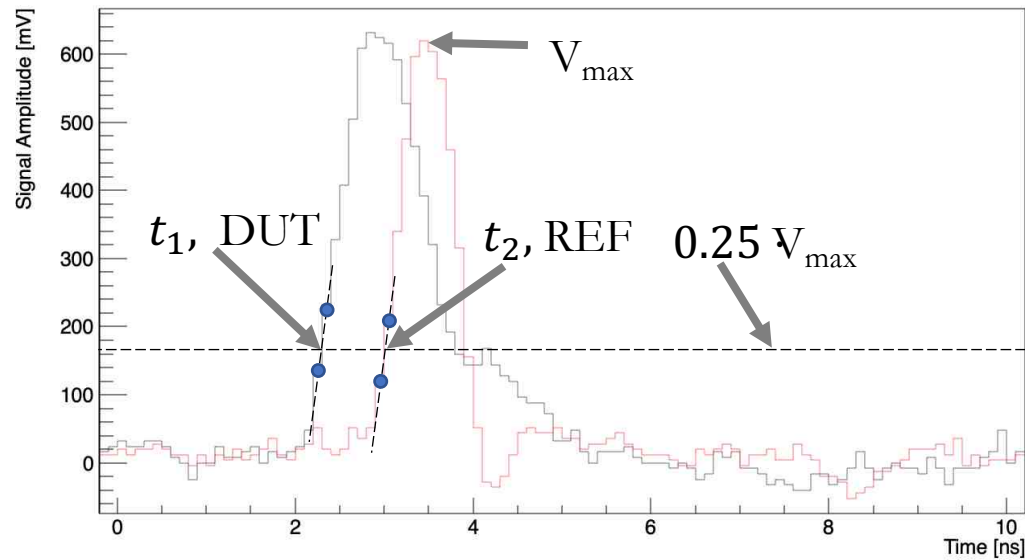
More neutron results in: A. Howard, LGAD measurements from different producers, 37th RD50 workshop

Beta Source Measurement: Charge Collection and Timing

- For charge collection and timing measurements, a timing reference LGAD (REF) and the device under test (DUT) are mounted on single channel readout boards developed by UCSC.
- Waveforms are read out on a Tektronix DPO 7254 Oscilloscope with 2.5GHz bandwidth.
- We use the shortest cables between the UCSC boards and oscilloscope for the best S/N performance and a Silicon Photomultiplier (SiPM) for triple coincidence.

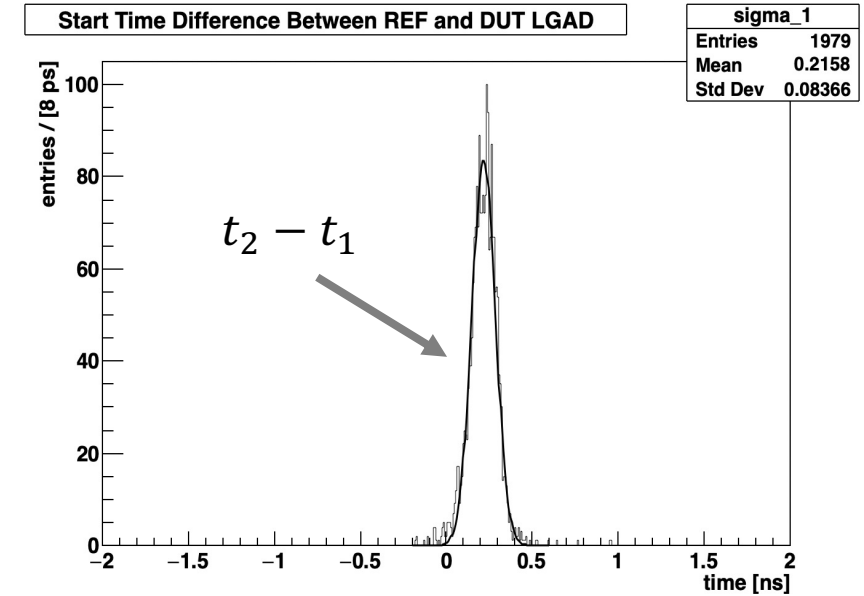
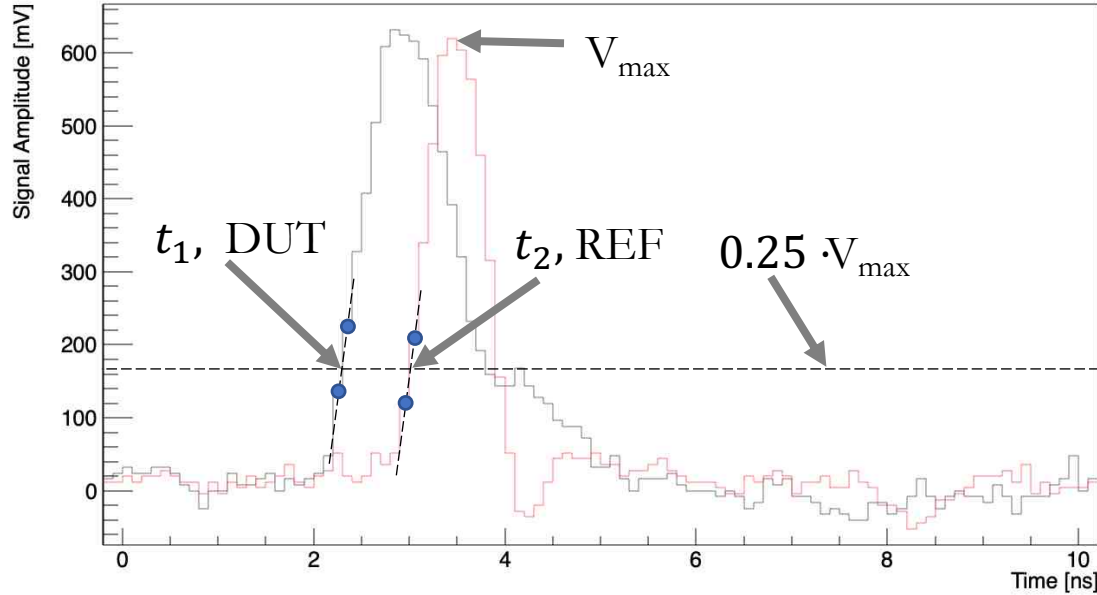


Beta Source Measurement: Charge Collection



- The REF and DUT waveforms are recorded for 2000 events.
- The amplitude of the DUT waveform is collected and binned. A Landau convolved with a gaussian is fit to the resulting distribution to extract the Most Probable Voltage (MPV).
- The MPV is converted to charge collection based on a calibration using a reference capacitor built into the UCSC board.

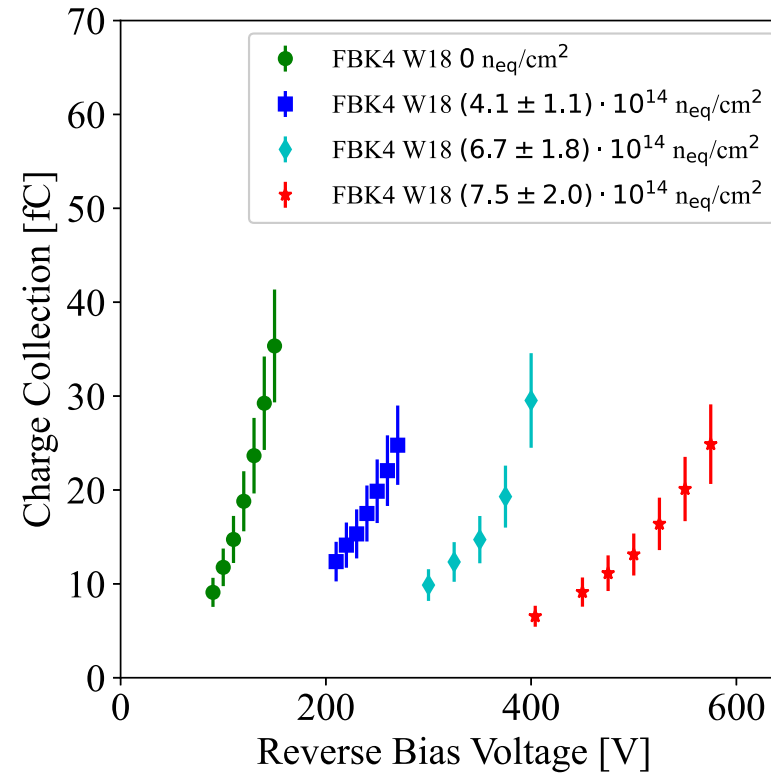
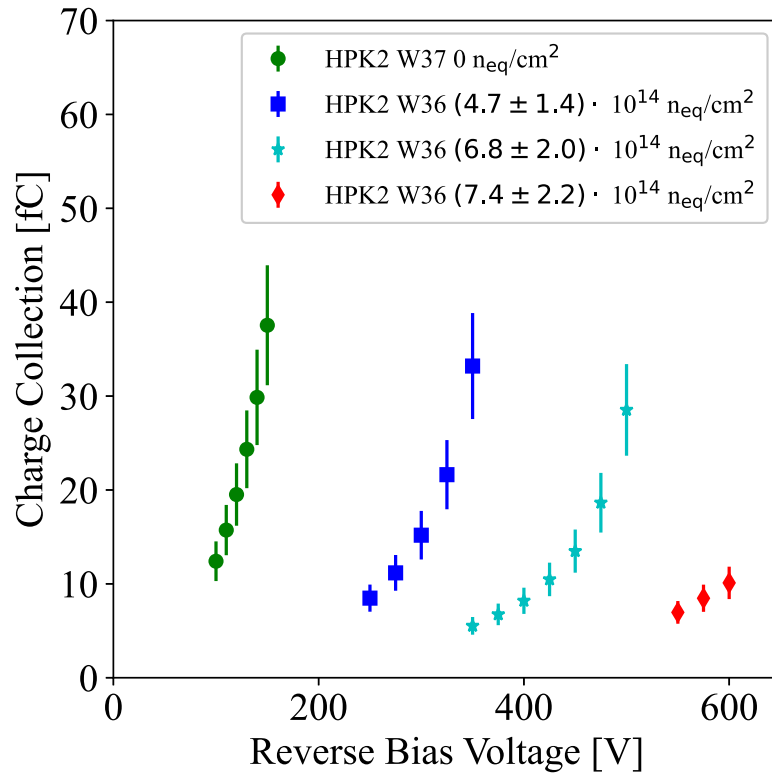
Beta Source Measurement: Timing



- The difference between the time over threshold of the REF and DUT sensors is binned. The standard deviation of the distribution is due to the timing resolution of the two LGADs, according to

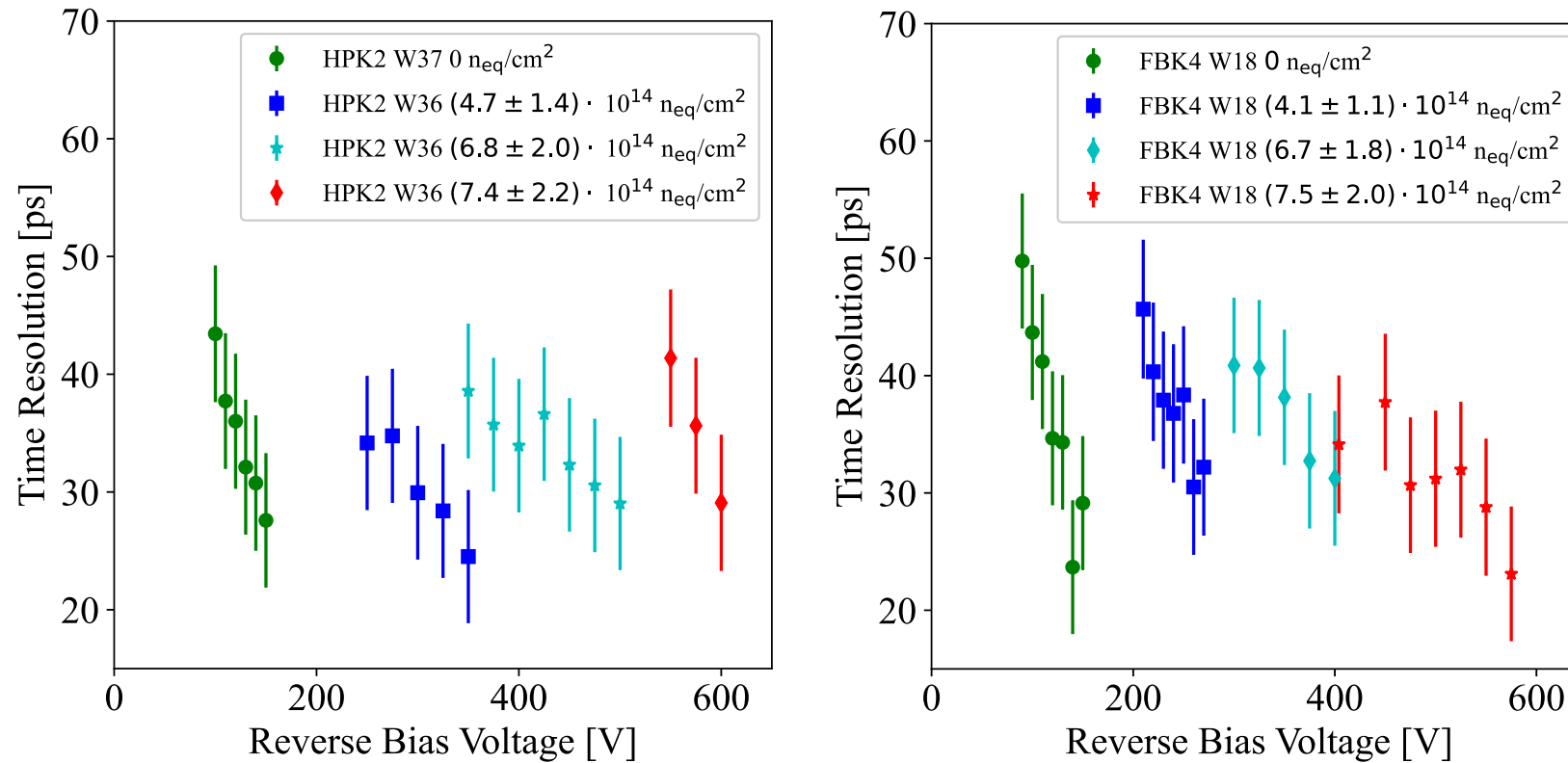
$$\sigma_{measured}^2 = \sigma_{DUT}^2 + \sigma_{REF}^2$$

Charge Collection Comparison



- The charge collection for the FBK4 wafer was higher than for the HPK2 wafer for comparable fluences and voltages.
- The FBK4 wafers irradiated higher than $11 \cdot 10^{14} \text{neq/cm}^2$ have no measurable charge collection below 600 V.

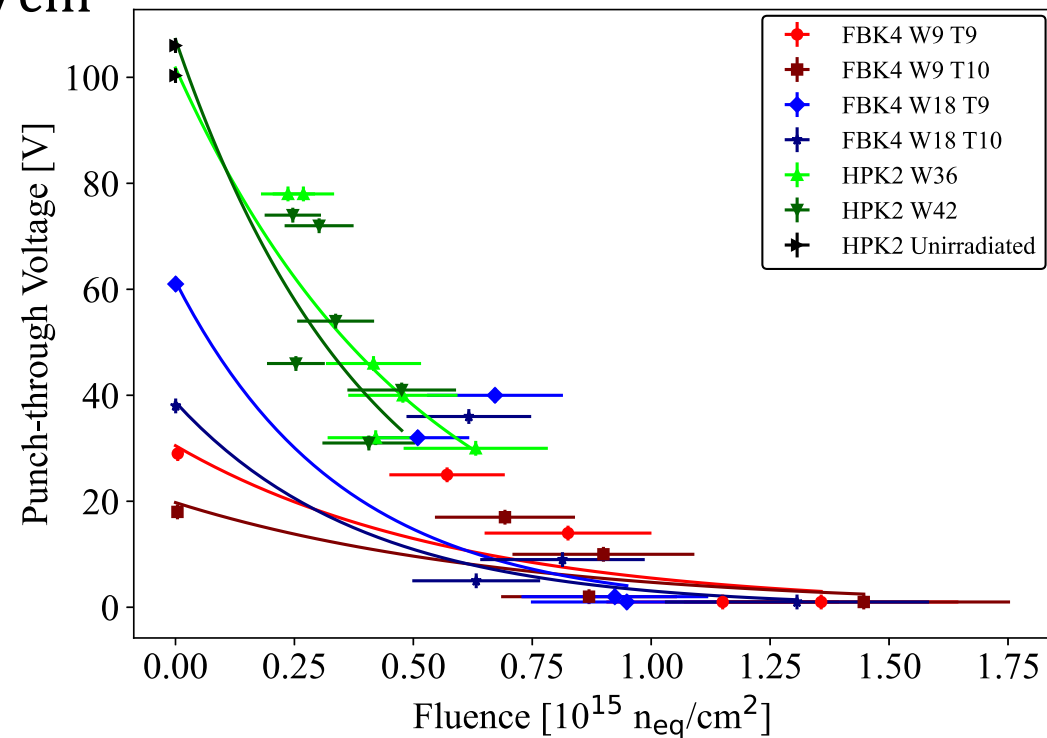
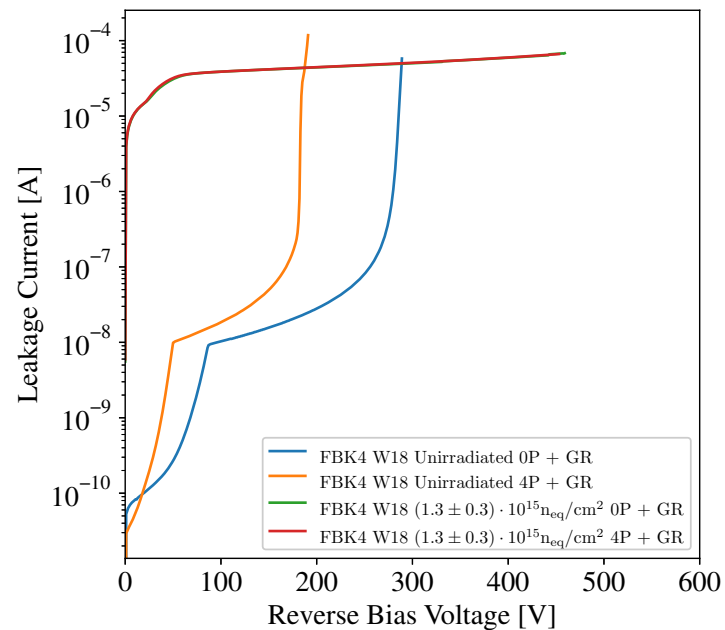
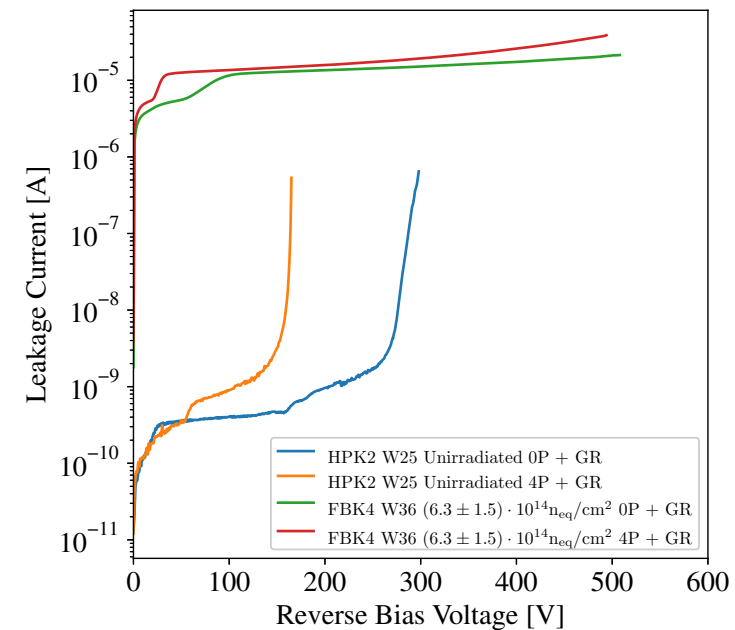
Timing Comparison



- Both sensors have timing resolution less than 70 ps for all measurements when the charge collection is above the 10 fC.
- The sensors irradiated above $10^{15} \text{ n}_{\text{eq}}/\text{cm}^2$ had no measurable charge collection and therefore no timing results.

Inter-electrode isolation measurements

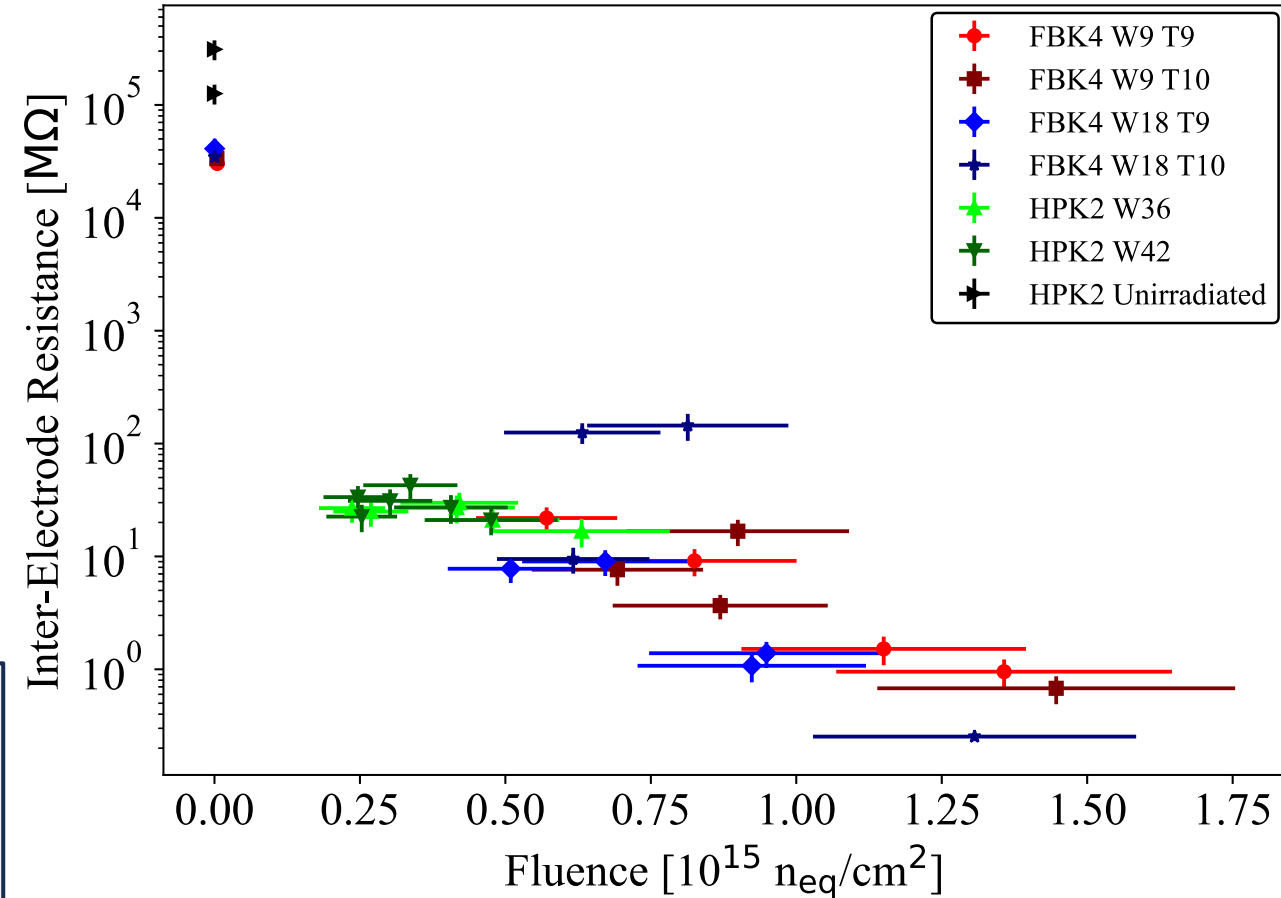
- Complementary measurements of the 2x2 LGADs with only the guard ring biased (0P+GR) and with all four pads biased (4P+GR) are used to extract the punch-through voltage.
- A decrease in punch-through voltage shows a decrease in the inter-electrode resistivity which increases the risk of cross talk between sensors.
- The punch-through voltage dropped to 0 V after $\sim 10^{15} n_{eq}/cm^2$



Direct measurement of the inter-electrode resistance

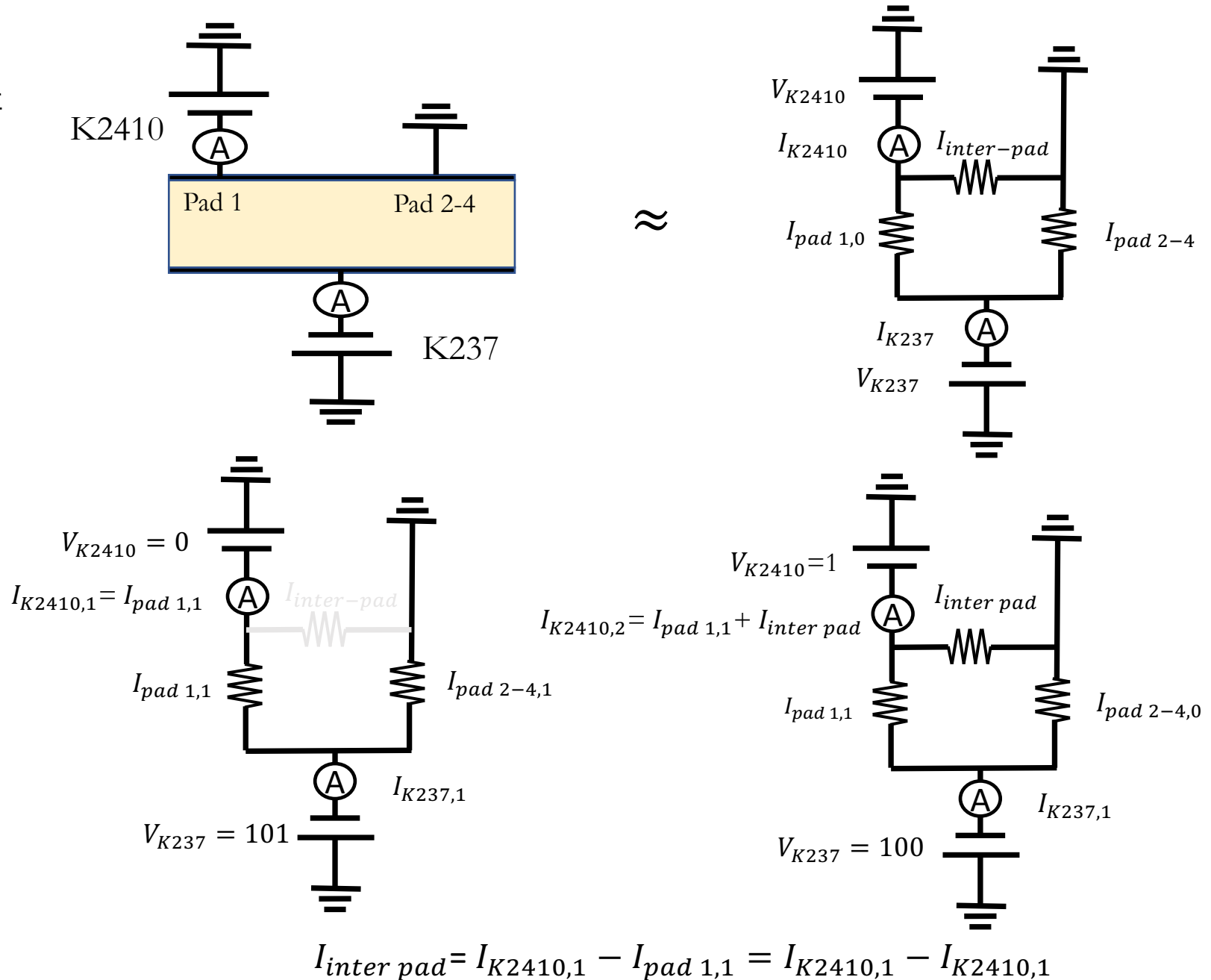
- A direct measurement of the inter-electrode resistance was made by grounding 3 pads and the guard ring, and then biasing the fourth electrode slightly above and below the ground.
- The measurement was made with the backside of the sensors at -100 V so the sensor is fully depleted.
- The inter-electrode resistance drops below $10\text{ M}\Omega$ after $\sim 10^{15}\text{ n}_{\text{eq}}/\text{cm}^2$

Despite the drop in punch-through voltage and inter-electrode resistance, direct measurements of the charge collection using a pulsed 1064 nm laser showed no evidence of cross talk even with low inter-electrode resistance.



Direct measurement of the inter-electrode resistance schematic

- The inter-electrode current measurement was performed with the amp-meters in a configuration shown in the top left figure.
- This configuration is approximately equivalent to the circuit diagram in the top right figure.
- By measuring in two different modes, shown in the bottom left and bottom right figures, the inter-pad current can be calculated without contribution from the bulk current.

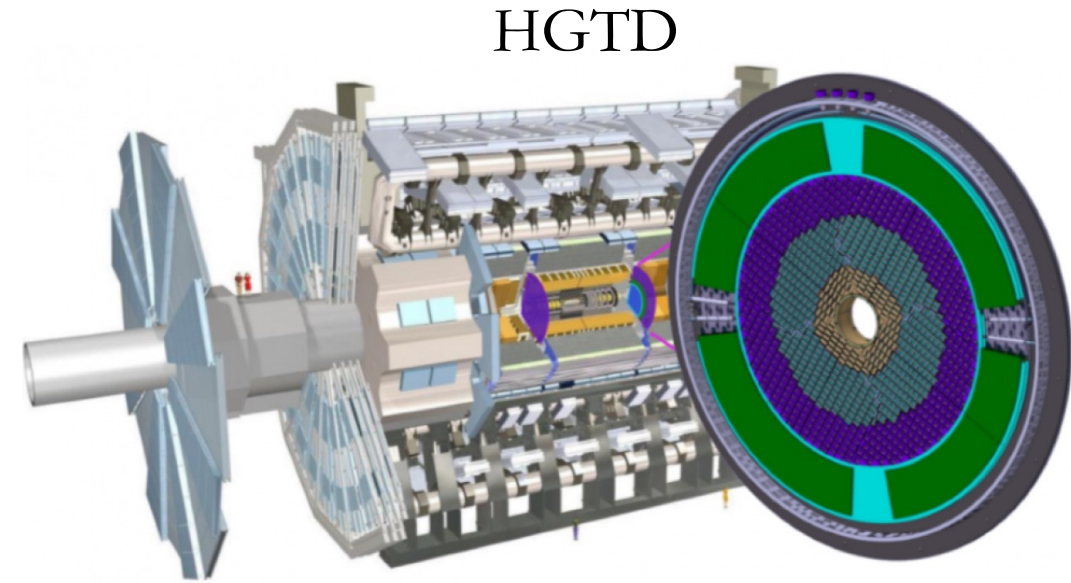


Summary

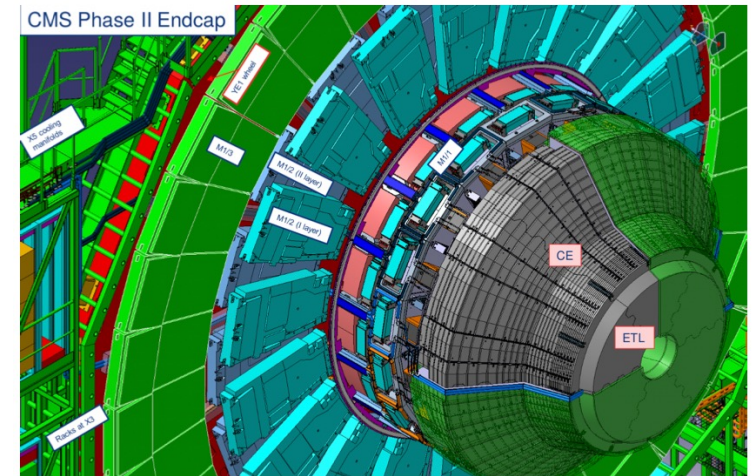
1. We carried out two proton irradiation campaigns of LGAD sensors produced by FBK and HPK.
2. Measurements on these proton irradiated LGADs of the leakage current, V_{gl} , $V_{breakdown}$, charge collection, timing resolution, and inter-electrode characteristics were made up to 600 V.
3. The acceptor removal constant for the proton irradiated LGADs is greater than for comparable neutron irradiated LGADs, even when the fluence is scaled with the NIEL hypothesis.
4. Both the FBK4 and HPK2 wafers reach < 35 ps and charge collection >10 fC up to $\sim 7 \cdot 10^{14} n_{eq}/cm^2$, but the FBK4 wafers reach the required charge collection with lower voltage.
5. Inter-electrode isolation of both HPK and FBK deteriorates as fluence increases. However, no cross-talk between the sensors was observed using a 1060 nm pulsed laser.

Motivation

- The HL-LHC will increase the luminosity by a factor of ~ 10 . The increased luminosity will increase the likelihood of tracks being miss-assigned, particularly in the forward region.
- To mitigate the misassignment, the High Granularity Timing Detector (HGTD) and Endcap Timing Layer (ETL) are being installed in ATLAS and CMS respectively. These timing layers have track timing resolution goals of 35 ps at the beginning of the lifetime and 70 ps at the end of the HL-LHC.
- The HGTD and ETL will be made of LGADs. The LGADs will need to operate after fluences up to $2.5 \cdot 10^{15} n_{eq}/cm^2$ (including a safety factor of 1.5).
- The LGADs' survivability to the radiation is the subject of this talk.



ETL

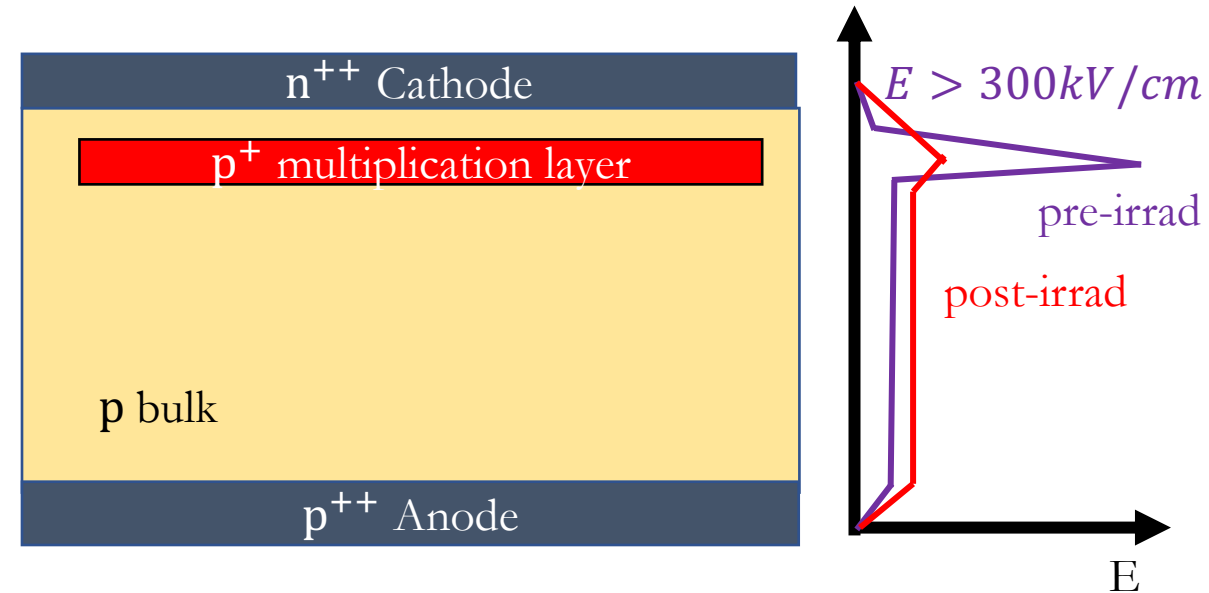


How LGADs work, and how LGADs are damaged

- LGADs are much thinner than conventional silicon sensors. Using thinner sensors creates temporally narrow signals with faster rise times, but reduces the charge collection.
- The reduced charge collection is counteracted by implanting a heavily doped layer, **the gain layer**. The gain layer concentrates the electric field to levels high enough for charge multiplication via impact ionization.
- The gain layer is sensitive to high-fluence, and deactivation of the boron dopant reduces the charge multiplication and renders the sensors ineffective.
- Different properties of the gain layer have effects on the radiation hardness, including the gain layer's depth, width, boron dopant concentration, and carbon co-implantation.

$$\sigma_t^2 = \sigma_{\text{jitter}}^2 + \sigma_{\text{time walk}}^2 + \sigma_{\text{landau}}^2$$

$$\sigma_{\text{time walk}} \propto \text{Rise Time} \quad \sigma_{\text{jitter}} = \frac{\text{Noise} \cdot \text{Rise Time}}{\text{Signal}}$$



$$V_{gl} = \frac{qN_A w^2}{2\epsilon}$$